A Novel Keystone Transform Based Algorithm for Moving Target Imaging with Radon Transform and Fractional Fourier Transform Involved

Jiefang Yang[1,2] **and Yunhua Zhang**[1]

[1]The Key Laboratory of Microwave Remote Sensing, Chinese Academy of Sciences, China
[2]University of Chinese Academy of Sciences, China

Abstract— In this paper, we propose a novel algorithm for SAR ground moving target imaging (SAR/GMTI) and motion parameters estimation (MPE) in consideration of Doppler ambiguity. This algorithm involves the keystone transform (KT) and the modified second-order keystone transform (MSKT), Radon transform (RT) and Fractional Fourier transform (FrFT). With this algorithm, the fast moving targets can be focused well and the motion parameters can be estimated accurately even in situation of Doppler ambiguity. The effectiveness of the proposed algorithm is demonstrated by processing the simulated airborne SAR data.

1. INTRODUCTION

Synthetic aperture radar ground moving target imaging (SAR/GMTI) is widely used in both civilian and military applications. There are various algorithms proposed for dealing with moving targets [1–3]. The keystone transform (KT) [1] and the second-order KT (SKT) [3] can be used to correct the RCM of moving targets without any prior knowledge required about their motion parameters. However, both KT and SKT suffer from the Doppler ambiguity problem. In real-world situations, Doppler ambiguity usually occurs for SAR imaging of fast moving target due to the limited PRF. In this paper, we propose an algorithm based on KT and Modified SKT (MSKT) for SAR/GMTI and MPE in Doppler ambiguity situation. This algorithm involves Radon transform (RT) [4] and Fractional Fourier transform (FrFT) [2] besides KT and MSKT. With this algorithm, the fast moving targets can be focused well and the motion parameters can be estimated accurately. The effectiveness of the proposed algorithm is demonstrated by processing the simulated airborne SAR data.

The remainder of the paper is organized as follows. In Section 2, we introduce the imaging model of an airborne SAR observing moving target and deduce the signal expression after range compression. In Section 3, we describe the proposed algorithm for moving target imaging and MPE. In Section 4, the simulated data is processed to show the effectiveness of the proposed algorithm. Finally, conclusion is drawn in Section 5.

2. THE IMAGING MODEL AND SPECTRUM ANALYSIS

The geometry of a broadside SAR observing a moving target is shown in Fig. 1. We use the LFM signal as the transmitted signal, so the baseband echo can be expressed as [5]:

$$s(\tau,\ \eta) = \sigma \mathrm{rect}\left[\frac{\tau - 2R(\eta)/c}{T_p}\right] \mathrm{rect}\left(\frac{\eta}{T_a}\right) \exp\left\{-j\frac{4\pi f_c}{c}R(\eta) - j\pi K\left(\tau - \frac{2R(\eta)}{c}\right)^2\right\} \tag{1}$$

where $R(\eta)$ denotes the instantaneous slant range between radar and target, A denotes an arbitrary complex constant, τ and η represent range-time and azimuth-time, respectively. T_p, f_c and K represent the time duration, carrier frequency and slope of the transmitted LFM signal, respectively. T_a denotes the target exposure time in azimuth.

According to Fig. 1, $R(\eta)$ can be expressed as follows:

$$\begin{aligned} R(\eta) &= \sqrt{(y_0 + v_y\eta)^2 + (V - v_x)^2\eta^2 + H_0^2} \approx R_0 + \alpha\eta + \beta\eta^2 + \chi\eta^3 \\ \text{and} &\quad \left\{\begin{array}{ll} R_0 = \sqrt{y_0^2 + H_0^2}, & \alpha = v_y \sin\vartheta \\ \beta = \frac{(V-v_x)^2 + v_y^2\cos^2\vartheta}{2R_0}, & \chi = -\frac{v_y \sin\vartheta\cdot\left[(V-v_x)^2 + v_y^2\cos^2\vartheta\right]}{2R_0^2} \end{array}\right. \end{aligned} \tag{2}$$

where, V and H_0 denote the velocity and height of the radar platform, v_x and v_y denote the along-track velocity and across-track velocity of the target, respectively, y_0 denotes the ground range of the moving target perpendicular to projection of the flight track, ϑ denotes the incident angle of SAR antenna, and $\sin\vartheta = y_0/R_0$.

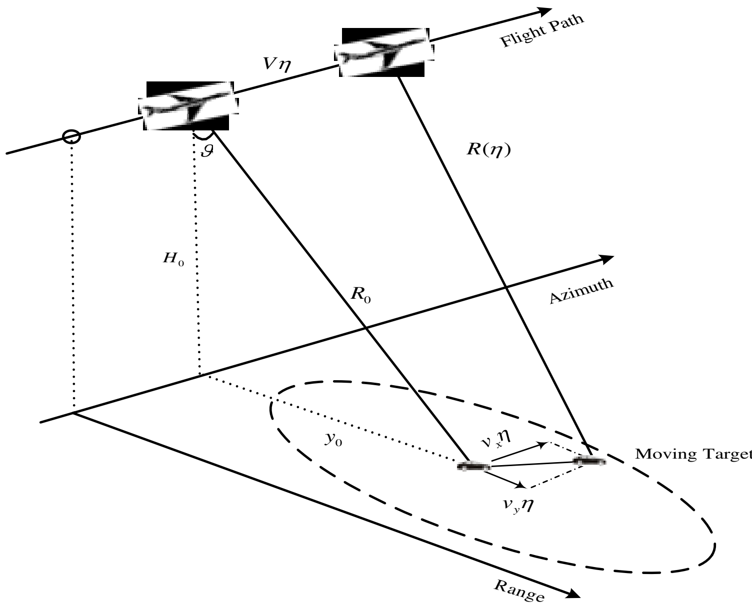

Figure 1: The geometry of SAR observing a moving target.

Suppose $\mu = f_\tau/f_c$ ($\mu \ll 1$, since $f_\tau \ll f_c$ is valid for general SAR), the output of range matched filtering in (f_τ, η) domain is expressed as:

$$S(f_\tau,\eta) = G(f_\tau,\eta)\exp\left\{-j\frac{4\pi f_c}{c}(1+\mu)\alpha\eta\right\}\exp\left\{-j\frac{4\pi f_c}{c}(1+\mu)\beta\eta^2\right\}\exp\left\{-j\frac{4\pi f_c}{c}(1+\mu)\chi\eta^3\right\} \tag{3}$$

where $G(f_\tau,\eta) = \sigma\mathrm{rect}\left(\frac{f_\tau}{KT_p}\right)\mathrm{rect}\left(\frac{\eta}{T_a}\right)\exp\left\{-j\frac{4\pi f_c}{c}(1+\mu)R_0\right\}$.

Suppose $\alpha = \alpha_0 + n\alpha_{prf}$, α_0 corresponds to the ambiguous Doppler centroid, n denotes the PRF fold factor and $\alpha_{prf} = c\mathrm{PRF}/(2f_c)$, then the second term in (3) can be expressed as following:

$$\exp\left\{-j\frac{4\pi f_c}{c}(1+\mu)\alpha\eta\right\} = \exp\left\{-j\frac{4\pi f_c}{c}(1+\mu)\alpha_0\eta\right\}\exp\left\{-j\frac{4\pi f_c}{c}\mu n\cdot\alpha_{prf}\eta\right\} \tag{4}$$

In (4) we omit the phase term $\exp\left\{-j\frac{4\pi f_c}{c}n\alpha_{prf}\eta\right\} = \exp\{-j2\pi n\mathrm{PRF}\eta\} = 1$.

3. THE PROPOSED ALGORITHM

In this section, we will present the proposed algorithm for moving target imaging and MPE. We first conduct KT on (3) to correct the range walk induced by the ambiguous Doppler centroid. KT is substituting the azimuth-time η with the expression $\eta = \left(\frac{f_c}{f_c+f_\tau}\right)\xi = \frac{1}{1+\mu}\xi$ [1]. After KT, the signal in (3) is changed to:

$$\begin{aligned} S_1(f_\tau,\xi) \;=\; & G(f_\tau,\xi)\exp\left\{-j\frac{4\pi f_c}{c}\alpha_0\xi\right\}\exp\left\{-j\frac{4\pi f_c}{c}\frac{\mu}{1+\mu}n\cdot\alpha_{prf}\xi\right\} \\ & \exp\left\{-j\frac{4\pi f_c}{c}\frac{\beta}{1+\mu}\xi^2\right\}\exp\left\{-j\frac{4\pi f_c}{c}\frac{\chi}{(1+\mu)^2}\xi^3\right\} \end{aligned} \tag{5}$$

Next, we will use (6) in the following to correct the range walk induced by the integer PRF ambiguity, and estimate n as done in [6], we will not repeat here.

$$H_1(f_\tau,\xi) = \exp\left(j\frac{4\pi f_c}{c}\frac{\mu}{1+\mu}n\cdot\alpha_{prf}\xi\right) = \exp\left(j2\pi\frac{f_\tau}{f_c+f_\tau}n\cdot PRF\xi\right) \tag{6}$$

By multiplying (5) with (6), the signal is expressed as following:

$$S_2(f_\tau,\xi)=G(f_\tau,\xi)\exp\left\{-j\frac{4\pi f_c}{c}\alpha_0\xi\right\}\exp\left\{-j\frac{4\pi f_c}{c}\frac{\beta}{1+\mu}\xi^2\right\}\exp\left\{-j\frac{4\pi f_c}{c}\frac{\chi}{(1+\mu)^2}\xi^3\right\} \tag{7}$$

In the following, let us conduct MSKT on (7) for range curvature correction, which is substituting ξ with the expression $\xi=\sqrt{1+\mu}\varsigma=\sqrt{1+\frac{f_\tau}{f_c}}\varsigma=\sqrt{\frac{f_c+f_\tau}{f_c}}\varsigma$. After applying the MSKT, the signal becomes as,

$$S_3(f_\tau,\varsigma)=G(f_\tau,\varsigma)\exp\left\{-j\frac{4\pi}{c}\left(f_c+\frac{f_\tau}{2}\right)\alpha_0\varsigma\right\}\exp\left\{-j\frac{4\pi f_c}{c}\beta\varsigma^2\right\}\exp\left\{-j\frac{4\pi}{c}\left(f_c-\frac{f_\tau}{2}\right)\chi\varsigma^3\right\} \tag{8}$$

where the approximations $\sqrt{1+\mu}\approx 1+\mu/2$ and $1/\sqrt{1+\mu}\approx 1-\mu/2$ are applied.

After transforming (8) to $(\tau,\,\varsigma)$ domain through range IFFT, the signal can be expressed as following:

$$\begin{aligned} s_3(\tau,\varsigma) &= A\mathrm{rect}\left(\frac{\varsigma}{T_a}\right)\mathrm{sinc}\left(KT_p\left(\tau-\frac{2R_0}{c}-\frac{\alpha_0}{c}\varsigma+\frac{\chi}{c}\varsigma^3\right)\right)\\ &\quad \exp\left\{-j\frac{4\pi f_c}{c}\alpha_0\varsigma\right\}\exp\left\{-j\frac{4\pi f_c}{c}\beta\varsigma^2\right\}\exp\left\{-j\frac{4\pi f_c}{c}\chi\varsigma^3\right\} \end{aligned} \tag{9}$$

Since $|\chi|\ll|\alpha_0|$ is usually valid, the target trajectory can be treated as an inclined line with a fix slope along the azimuth dimension. We can estimate the slope using RT, and thus obtain the estimation of α_0, denoted by α_0^{est} [4]. At this time, we can obtain the estimation of α as $\alpha^{est}=\alpha_0^{est}+n\cdot\alpha_{prf}$, and construct the correction function for range walk and Doppler shift as following:

$$H_2(f_\tau,\,\varsigma)=\exp\left\{j\frac{4\pi f_c}{c}\alpha_0^{est}\varsigma+j\frac{2\pi f_\tau}{c}\alpha_0^{est}\varsigma\right\} \tag{10}$$

Let us multiply (8) with (10) and do range IFFT, the signal in (τ,ς) domain is expressed as,

$$s_4(\tau,\varsigma)=Arect\left(\frac{\varsigma}{T_a}\right)\mathrm{sinc}\left(KT_p\left(\tau-\frac{2R_0}{c}\right)\right)\exp\left\{-j\frac{4\pi f_c}{c}\beta\varsigma^2\right\}\exp\left\{-j\frac{4\pi f_c}{c}\chi\varsigma^3\right\} \tag{11}$$

Eqaution (11) shows that, the energy of the moving target is concentrated in a single range cell. Here, we can extract the moving target azimuthal signal and estimate the Doppler rate through FrFT [2], denoted by K_d^{est}, and then we can obtain the estimation of β as $\beta^{est}=-cK_d^{est}/4f_c$. We should indicate that the third-order phase term is treated as clutter in the implementation of FrFT. In the following, we can calculate the motion parameters as,

$$v_y^{est}=\alpha^{est}/\sin\vartheta,\quad \text{and}\quad v_x^{est}=V-\sqrt{2R_0\beta^{est}-\left(v_y^{est}\cos\vartheta\right)^2} \tag{12}$$

At present, we can construct the azimuth matched filter function $H_a(f_\xi)$ and the third-order phase compensation function $H_4(f_\tau,\xi)$ as follows,

$$H_a(f_\xi)=\exp\left\{j\pi\frac{cf_\xi^2}{4f_c\beta^{est}}\right\},\quad \text{and}\quad H_4(f_\tau,\xi)=\exp\left\{j\frac{4\pi f_c}{c}\left(1-\frac{f_\tau}{2f_c}\right)\chi^{est}\xi^3\right\} \tag{13}$$

After azimuth matched filtering and compensation of the third-order phase to (11), the final image of the moving target in $(\tau,\,\xi)$ domain can be obtained as following:

$$s_{ac}(\tau,\,\xi)=A\mathrm{sinc}\left[KT_p\left(\tau-\frac{2R_0}{c}\right)\right]\cdot\mathrm{sinc}\left(\frac{4\beta^{est}}{\lambda}T_a\xi\right) \tag{14}$$

4. SIMULATION

In this section, we will conduct simulations to validate the proposed algorithm. In real situations, there exist nonlinear motions for the SAR platform. However, these motion errors can be well compensated by the existing methods [7]. After the motion compensation, the proposed algorithm can be used to deal with the moving targets. Therefore, the motion errors of the SAR platform are not taken into consideration in this simulation. The simulation system parameters are listed in Table 1. There are three moving targets in the scene, T_1 is a slowly moving target without inducing Doppler ambiguity, while T_2 and T_3 are fast moving targets with Doppler ambiguity induced. The true motion parameters of the targets and the estimated motion parameters with the proposed algorithm are listed in Table 2, it is clear that our algorithm can achieve accurate MPE. Fig. 2

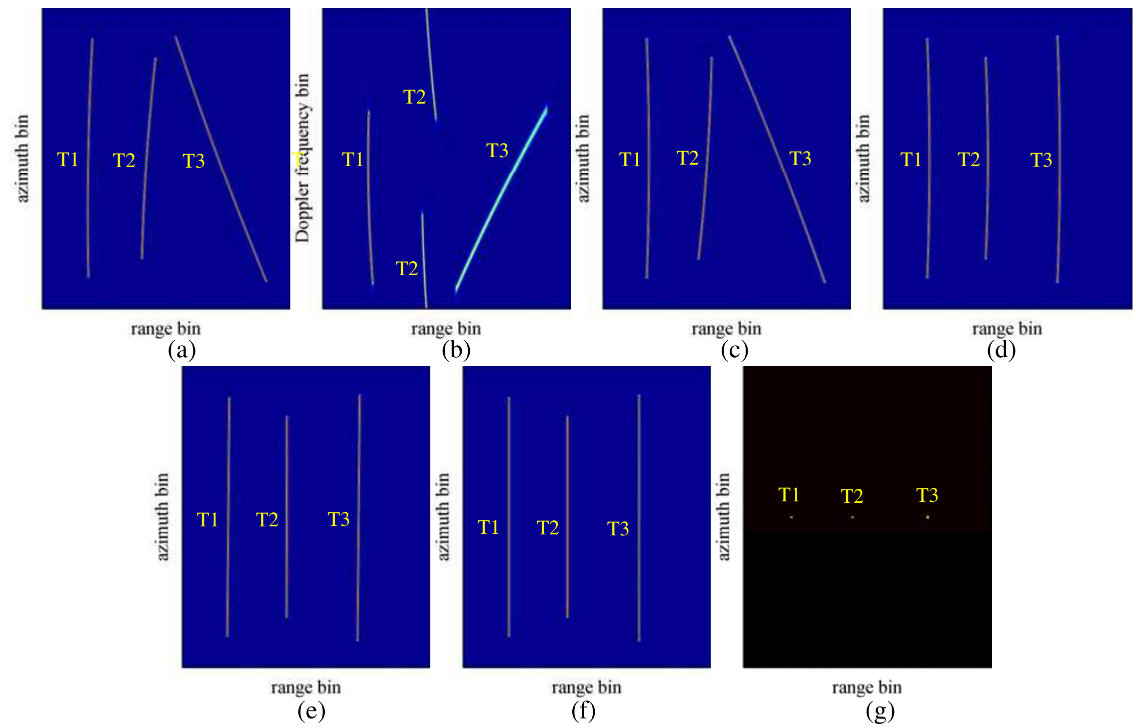

Figure 2: The procedure of the proposed algorithm. (a) The target trajectories after range compression, which shows that the range walk and range curvature for the three targets are different. (b) The Doppler spectrums after range compression, the spectrum of T_2 is split into two parts. (c) The result of KT, which shows that the range walk of T_1 is corrected, while the range walks of T_2 and T_3 still exist due to the integer PRF ambiguity. (d) The result after integer PRF ambiguity compensated for T_2 and T_3, which shows that there are only range curvatures left. (e) The result of applying MSKT, which shows that the range curvatures for each target are corrected. (f) The result of range walks correction after using RT to estimate the slope, which shows that the energy of each target is concentrated in a corresponding range cell. (g) The final focused image after using FrFT to estimate the Doppler rate and then having the azimuthal signals compressed.

Table 1: The simulation system parameters.

carrier frequency f_c	bandwidth B	pulse duration T_p	range sampling rate F_s	incident angle ϑ
14.0 GHz	200 MHz	5 us	250 MHz	45°
azimuth beamwidth	PRF	platform velocity V	platform height H_0	
3°	1000	120m/s	5000m	

Table 2: The simulated targets motion parameters.

Targets	R_0(m)	v_y(m/s)	v_y^{est}(m/s)	Relative error	v_x(m/s)	v_x^{est}(m/s)	Relative error
T_1	7007	2	1.99	0.5%	3	2.97	1%
T_2	7071	8	8.00	0	−20	−19.98	0.1%
T_3	7149	−43	−42.99	0.02%	4	3.60	10%

presents the result of each step of the proposed algorithm until the final image is obtained, obviously, they are very well focused, i.e., the effectiveness of the proposed algorithm is demonstrated.

5. CONCLUSION

In this paper, we propose an algorithm for SAR/GMTI and MPE. In this algorithm, the KT, the MSKT, the RT and the FrFT are utilized. With this algorithm, the fast moving targets can be well focused and their motion parameters can be estimated accurately even with the Doppler ambiguity involved. The effectiveness of the proposed algorithm is validated by processing the simulated airborne SAR data.

REFERENCES

1. Perry, R. P., R. C. DiPietro, and R. L. Fante, "SAR imaging of moving targets," *IEEE Transactions on Aerospace and Electronic Systems*, Vol. 35, No. 1, 188–200, 1999.
2. Sun, H., G. S. Liu, H. Gu, and W. M. Su, "Application of the fractional Fourier transform to moving target detection in airborne SAR," *IEEE Transactions on Aerospace and Electronic Systems*, Vol. 38, No. 4, 1416–1424, 2002.
3. Zhou, F., R. Wu, M. Xing, and Z. Bao, "Approach for single channel SAR ground moving target imaging and motion parameter estimation," *IET Radar Sonar and Navigation*, Vol. 1, No. 1, 59–66, 2007.
4. Warrick, A. L. and P. A. Delaney, "Detection of linear features using a localized radon transform," *Conference Record of the Thirtieth Asilomar Conference on Signals, Systems and Computers*, 1245–1249, 1996.
5. Cumming, I. G. and F. H. Wong, *Digital Signal Processing of Synthetic Aperture Radar Data: Algorithms and Implementation*, Artech House Norwood, 2004.
6. Su, J., M. Xing, G. Wang, and Z. Bao, "High-speed multi-target detection with narrowband radar," *IET Radar Sonar and Navigation*, Vol. 4, No. 4, 595–603, 2010.
7. Carrar, W. G., R. S. Goodman, and R. M. Majewski, *Spotlight Synthetic Aperture Radar-signal Processing Algorithm*, Artech House, Norwood, MA, 1995.